Synthesis and Conformational Characterization of Tethered, Self-Complexing 1,5-Dialkoxynaphthalene/ 1,4,5,8-Naphthalenetetracarboxylic Diimide Systems

Andrew J. Zych and Brent L. Iverson*

Contribution from the Department of Chemistry and Biochemistry The University of Texas at Austin, Austin, Texas 78712

Received May 31, 2000

Abstract: Chemists are beginning to explore the abiotic folding of synthetic chains, and the term "foldamers" has been used to characterize oligomers with a strong inclination to adopt specific, compact conformations. The characterization of folded structure in solution is one of the difficult challenges facing the foldamer field. Aedamers were the first foldamers to make use of aromatic−aromatic interactions in water to direct folding and were designed to have several spectroscopic handles with which to probe folding conformations in solution. Herein is reported the synthesis and spectroscopic characterization of eleven aedamer dimers, with linkers chosen to provide a spectrum of lengths and flexibilities. The dimers, composed of one electron rich (1,5-dialkoxynaphthalene) and one electron deficient (1,4,5,8-naphthalenetetracarboxylic diimide) aromatic group tethered by a linker, are the smallest aedamer folding unit. The powerful spectroscopic handles associated with the stacked aedamer groups were exploited in a comprehensive spectroscopic analysis of conformation that included UV−vis absorption spectroscopy, fluorescence measurements (including time-resolved studies), as well as detailed NMR studies. The spectra were interpreted in the context of molecular modeling/spectral prediction and structural models were developed for the different dimers in aqueous solution. In most instances, the observed data was best described by an ensemble of predicted structures as opposed to one or few conformers. Thus, in the case of these aedamer dimers, "folding" does not appear to imply a two-state model with a rigid, unique conformation. Rather, the reported analysis indicates the data can best be described by a more dynamic model in which a given molecule spends its time in different folded conformations that are related by having a characteristic face-to-face stacking arrangement of the aromatic units.

Introduction

Inspired by the remarkable variety of molecular architectures found among biological macromolecules such as proteins and nucleic acids, the synthesis of oligomers with predictable secondary structure has attracted increasing interest in recent years.[1] Natural macromolecules are composed of linear chains folded into compact structures, producing three-dimensional ensembles of functional groups capable of complex tasks such as binding and/or catalysis. Chemists are beginning to explore abiotic folding of synthetic chains, and the term "foldamers" has been used to characterize oligomers with a strong inclination to adopt a specific compact conformation.[1a] Examples of foldamers include β-peptides,[2] γ-peptides,[3] vinylogous peptides,[4] sulfonopeptides,[5] peptoids,[6] oligocarbamates,[7] oligopyrrolidones,[8] oligoureas,[9] carbohydrate oligomers,[10] oligoanthrilamides,[11a,b] crescent oligoamides,[11c] meta-linked phenylacetylenes,[12] and pyrimidine−pyridine oligomers.[13] Hydrogen bonding, conformational restriction, and solvophobic interactions have all been used to advantage in the design of these folding molecular systems.

Aedamers were the first foldamers to make use of aromatic−aromatic interactions in water to direct folding.[14] The aedamer design is based on the face-to-face association of alternating electron-rich "donor", 1,5-dialkoxynaphthalene (DAN), and electron-deficient "acceptor", 1,4,5,8-naphthalenetetracarboxylic diimide (NDI), aromatic moieties. The aromatic units are connected by flexible linkages that are designed to allow a pleated structure with a stacked core of aromatic units (Figure 1a). In aqueous solution, this folding is assumed to have a large solvophobic driving force, which operates in concert with the **a**romatic **e**lectron **d**onor−**a**cceptor complexation upon which the **aeda**mer name is based. Initial investigations were performed on aedamers consisting of 2, 4, or 6 alternating aromatic units linked through aspartate residues (Figure 1b).

A key challenge facing the foldamer field is the characterization of folded conformation in solution. Aedamers possess a

* To whom correspondence should be addressed. E-mail: biverson@utxvms.cc.utexas.edu.

(1) (a) Gellman, S. H. *J. Acc. Chem. Res.* **1998**, *31*, 173. (b) Seebach, D.; Matthews, J. L. *Chem. Commun*. **1997**, 2015. (c) Iverson, B. L. *Nature* **1997**, *385*, 113. (d) Borman, S. *Chem. Eng. News* June 16 **1997**, 32.

(2) (a) Barchi, J. J.; Huang, X.; Appella, D. H.; Christianson, L. A.; Durell, S. R.; Gellman, S. H. *J. Am. Chem. Soc*. **2000** *122*, 2711−2718. (b) Appella, D. H.; Christianson, L. A.; Karle, I. L.; Powell, D. R.; Gellman, S. H. *J. Am. Chem. Soc*. **1999**, *121*, 6206. (c) Appella, D. H.; Barchi, J. J.; Durell, S. R.; Gellman, S. H. *J. Am. Chem. Soc*. **1999**, *121*, 2309. (d) Krauthäuser, S.; Christianson, L. A.; Powell, D. R.; Gellman, S. H. *J. Am. Chem. Soc*. **1997**, *119*, 11719. (e) Appella, D. H.; Christianson, L. A.; Klein, D. A.; Powell, D. R.; Huang, X.; Barchi, J. J.; Gellman, S. H. *Nature* **1997** *387*, 381. (f) Gademan, K.; Jaun, B.; Seebach, D. *Helv. Chim. Acta*. **1999**, *82*, 1. (g) Daura, X.; Gademan, K.; Jaun, B.; Seebach, D.; van Gunsteren, W. F.; Mark, A. E. *Angew. Chem., Int. Ed*. **1999**, *38*, 236. (h) Guichard, G.; Abele, S.; Seebach, D. *Helv. Chim. Acta*. **1998**, *81*, 187. (i) Seebach, D.; Abele, S.; Schrieber, J. V.; Martinoni, B.; Nussbaum, A. K.; Schild, H.; Schulz, H.; Hennecke, H.; Woessner, R.; Bitsch, F. *Chimia* **1998**, *52*, 734.

(3) (a) Hanessian, S.; Luo, X.; Schaum, R. *Tetrahedron Lett*. **1999**, *40*, 4925. (b) Hanessian, S.; Luo, X.; Schaum, R.; Michnick, S. *J. Am. Chem. Soc*. **1998**, *120*, 8569.

(4) Hagihara, M.; Anthony, N. J.; Stout, T. J.; Clardy, J.; Schreiber, S. L. *J. Am. Chem. Soc*. **1992**, *114*, 6568.

(5) Gennari, C.; Salom, B.; Potenza, D.; Williams, A. *Angew. Chem., Int. Ed. Engl*. **1994**, *33*, 2067.

10.1021/ja0019225 CCC: $19.00
Published on Web 08/31/2000

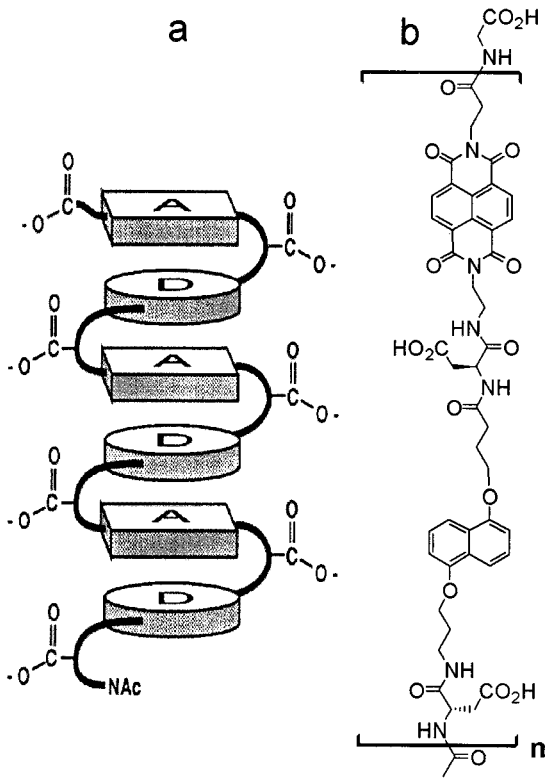

Figure 1. (a) Schematic representation of folded aedamer structure. (b) Chemical structure of aedamer oligomers.

number of powerful spectroscopic handles related to folding by virtue of the stacked aromatic units that comprise the core of the folded structure. In fact, inclusion of such spectroscopic handles was an important consideration in the original aedamer design. Nevertheless, a thorough understanding of aedamer folding is complicated by the size and flexibility of the molecules, especially the larger derivatives. Therefore, a series of investigations were undertaken to characterize details of folding in the smallest folding unit, namely the dimer, composed of one DAN and one NDI unit tethered by a linker. At the same time, it was of interest to see how differences in linker flexibility and length influence dimer folding.

Herein is reported the synthesis and spectroscopic characterization of 10 *folding* aedamer dimers, with linkers chosen to provide a spectrum of lengths and flexibilities (Figure 2). A control dimer, compound **11**, was also synthesized in which folding is prevented through geometric constraints. Additionally, water-soluble DAN and NDI monomers were synthesized and their interactions characterized. A combination of UV−vis absorption spectroscopy, fluorescence measurements (including time-resolved studies), NMR, and molecular modeling/spectra simulation are reported, enabling conclusions to be drawn regarding the degree of folding, as well as the types of folded conformations observed in the different molecules. Taken together, the results and accompanying analysis provide a comprehensive description of aedamer folding in solution, paving the way for future investigations into the solution structures of more complex aedamers and related foldamers.

Results

Monomer Studies. Water-soluble, uncharged analogues of DAN and NDI (Figure 3) were synthesized (see the Supporting Information). An NMR titration was carried out in D_2O in which the chemical shift of the NDI **12** aromatic protons was followed as a function of DAN **13** concentration.[15]

The NMR titration data was examined using a Scatchard analysis. Because of significant curvature apparent in the Scatchard plot (Figure 4a), a combination of 1:1 and 2:1 binding was postulated.[17] Thus, the binding isotherm was fit with an equation that includes the presence of both complexes (Figure 4b).[18] Association constants of 1300 ± 200 M^{-1} and 200 ± 100 M^{-1} were derived for the 1:1 and 2:1 complexes, respectively. The corresponding upfield chemical shift changes ($\Delta\delta$) of -0.42 ± 0.10 ppm and -0.84 ± 0.02 ppm were determined for the 1:1 and 2:1 complexes, respectively. Since the concentration of **12** was kept constant while **13** was increased, it is assumed that the 2:1 species corresponds to a **13**−**12**−**13** complex.[19]

Dimer Synthesis. Ten different *folding* aedamer dimers **1**−**10** were synthesized in an effort to provide a spectrum of linker length and rigidity. For example, dimers **1**−**5** have 0−4 amino acid residues between the DAN and NDI units. Dimers **6**−**8** are rigidified by virtue of having various bond rotations prevented by cyclic amino acid units, while dimer **9** has an overall cyclic structure. Dimer **10** is analogous to **2**, except that the N-terminus is not blocked with an acetamide group and the aspartate was moved to the C-terminus in order to examine the influence on folding of potential noncovalent cyclization due

(6) (a) Kirshenbaum, K.; Barron, A. E.; Goldsmith, R. A.; Armand, P.; Bradley, E. K.; Truong, K. T. V.; Dill, K. A.; Cohen, F. E.; Zuckermann, R. N. *Proc. Natl. Acad. Sci. U.S.A.* **1998**, *95*, 4303. (b) Armand, P.; Kirshenbaum, K.; Goldsmith, R. A.; Farr-Jones, S.; Barron, A. E.; Truong, K. T. V.; Dill, K. A.; Mierke, D. F.; Cohen, F. E.; Zuckermann, R. N.; Bradley, E. K. *Proc. Natl. Acad. Sci. U.S.A.* **1998**, *95*, 4309. (c) Armand, P.; Kirshenbaum, K.; Falicov, A.; Dunbrack, R. L.; Dill, K. A.; Zuckermann, R. N.; Cohen, F. E. *Fold. Design* **1997**, *2*, 369.

(7) (a) Paikoff, S. J.; Wilson, T. E.; Cho, C. Y.; Schultz, P. G. *Tetrahedron Lett*. **1996**, *37*, 5653. (b) Cho, C. Y.; Moran, E. J.; Cherry, S. R.; Stephans, J. C.; Fodor, S. P. A.; Adams, C. L.; Sundaram, A.; Jacobs, J. W.; Schultz, P. G. *Science* **1993**, *261*, 1303.

(8) Smith, A. B., III; Guzman, M. C.; Sprengeler, P. A.; Keenan, T. P.; Holcomb, R. C.; Wood, J. L.; Carroll, P. J.; Hirschmann, R. *J. Am. Chem. Soc*. **1994**, *116*, 9947.

(9) (a)Wilson, M. E.; Nowick, J. S.; *Tetrahedron Lett*. **1998**, *39*, 6613. (b) Nowick, J. S.; Mahrus, S.; Smith, E. M.; Ziller, J. W. *J. Am. Chem. Soc*. **1996**, *118*, 1066.

(10) Szabo, L.; Smith, B. L.; McReynolds, K. D.; Parrill, A. L.; Morris, E. R.; Gervay, J. *J. Org. Chem*. **1998**, *63*, 1074.

(11) (a) Hamuro, Y.; Geib, S. J.; Hamilton, A. D. *J. Am. Chem. Soc*. **1997**, *119*, 10587. (b) Hamuro, Y.; Geib, S. J.; Hamilton, A. D. *Angew. Chem. Int. Ed. Engl*. **1994**, *33*, 446. (c) Zhu, J.; R. D.; Zeng, H.; Skrzypczak-Jankun, E.; Zeng, X. C.; Gong, B. *J. Am. Chem. Soc*. **2000**, *122*, 4219.

(12) (a) Brunsveld, L.; Prince, R. B.; Meijer, E. W.; Moore, J. S. *Org. Lett.* **2000**, *2*, 1525. (b) Prince, R. B.; Okada, T.; Moore, J. S. *Angew. Chem., Int. Ed*. **1999**, *38*, 233. (c) Prince, R. B.; Saven, J. G.; Wolynes, P. G.; Moore, J. S *J. Am. Chem. Soc*. **1999**, *121*, 3114. (d) Nelson, J. C.; Saven, J. G.; Moore, J. S.; Wolynes, P. G *Science* **1997**, *277*, 1793.

(13) Bassani, D. M.; Lehn, J.-M.; Baum, G.; Fenske, D. *Angew. Chem., Int. Ed. Engl*. **1997**, *36*, 1845.

(14) (a) Lokey, R. S.; Iverson, B. L. *Nature* **1995**, *375*, 303. (b) Nguyen, J. Q.; Iverson, B. L. *J. Am. Chem. Soc*. **1999**, *121*, 2639.

(15) Significant self-association of the NDI derivative **12** was observed, estimated to be ~150 M^{-1} based on the concentration dependence of its NMR spectrum.[16] The DAN monomer **13** exhibited much less self-association with an NMR-estimated dimerization constant of ~10 M^{-1}. Note that both the NDI and DAN concentrations were kept low enough to avoid any significant complications due to self-association.

(16) Horman, I.; Dreux, B. *Helv. Chim. Acta* **1984**, *67*, 754.

(17) (a) Deranleau, D. A. *J. Am. Chem. Soc*. **1969**, *91*, 4050. (b) Tsukube, H.; Furuta, H.; Odani, A.; Takeda, Y.; Kudo, Y.; Inoue, Y.; Liu, Y.; Sakamoto, H.; Kimura, K. In *Comprehensive Supramolecular Chemistry*; Atwood, J. L., Lehn, J. M., Eds.; Pergamon Press: New York, 1996; Vol. 8, Chapter 10.

(18) (a) Chudek, J. A.; Foster, R.; Twiselton, D. R.; *J. Chem. Soc., Perkin Trans. 2* **1983**, 1385. (b) Dodson, B.; Foster, R.; Bright, A. A. S.; Foreman, M. I.; Gorton, J. *J. Chem. Soc. B* **1971**, 1283.

(19) Preliminary experiments suggested that a 2:1 complex of the form **12**−**13**−**12** could also be observed when the NDI **12** was in excess, but self-aggregation of **12** at higher concentrations precluded a meaningful quantitative analysis in this concentration regime.

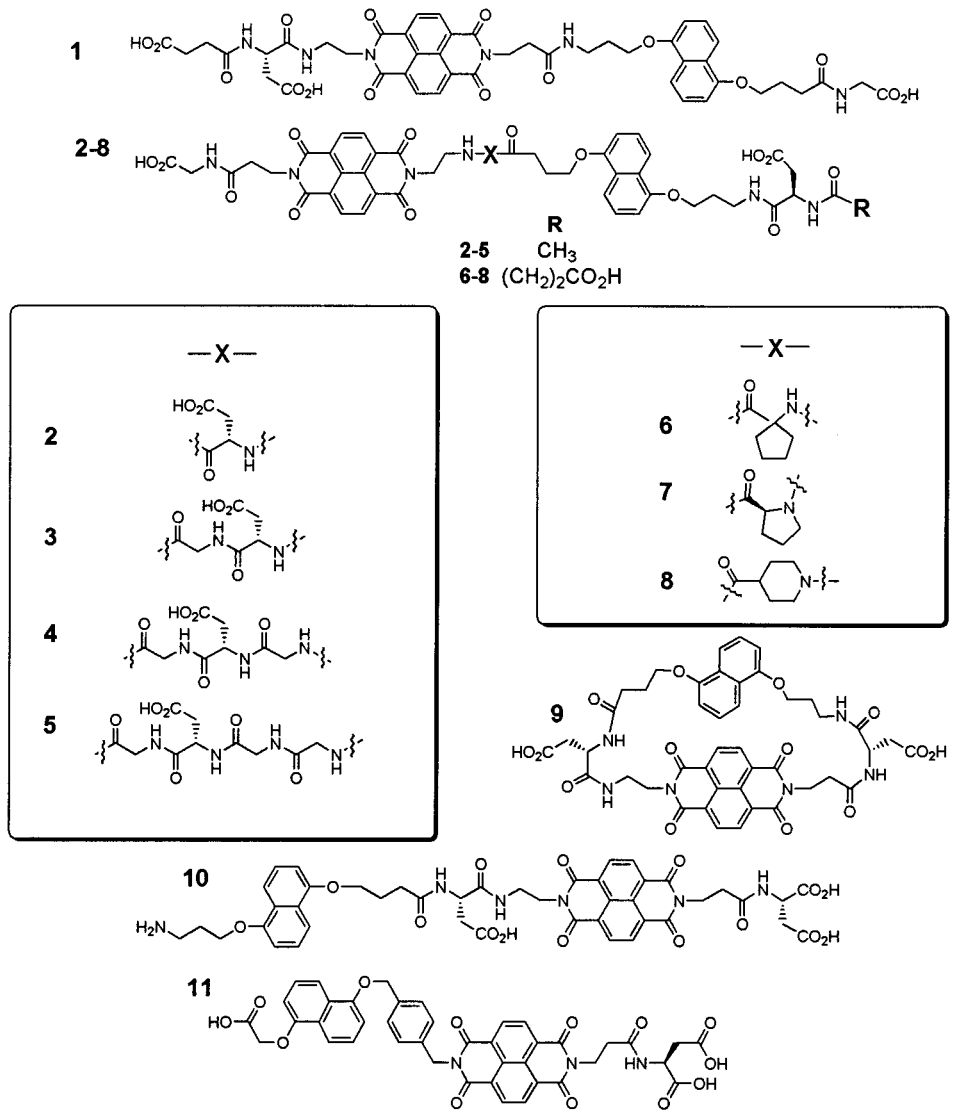

Figure 2. Aedamer dimers synthesized for this study. **11** is a control compound in which folding is prevented through geometric constraints.

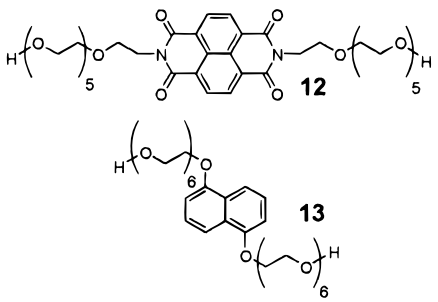

Figure 3. Neutral NDI (**12**) and DAN (**13**) compounds for NMR titrations.

to a putative salt bridge between terminal groups. As a control, compound **11**, which is precluded from folding by virtue of the geometric constraints imposed by the aromatic linker, was also synthesized.

The aedamer dimers **1**−**10** were synthesized using standard Fmoc-based solid-phase methodologies. The syntheses of DAN and NDI-containing amino acids for solid-phase coupling are included in the Supporting Information. Glycine-functionalized Wang resin was used for all compounds, except **9** and **10**, to provide a C-terminal glycine residue. Aspartic acid-functionalized Wang resin was used for **10**. For **9,** a Wang Tentagel resin was functionalized with Fmoc-Asp-ODmb to provide a handle for cyclization.[20] Dimers **2**−**5** were reacted with acetic anhydride to cap the N-terminus, as in the original aedamer design, while **6**−**8** were capped with succinic anhydride to replace the negative charge not present in the linkage. The synthesis of the control compound **11** is also included in the Supporting Information.

NMR Chemical Shift Changes. Chemical shift changes compared to the NDI **14** and DAN **15** reference compounds for signals common to the 10 *folding* dimers **1**−**10** are listed in Table 1. Spectra were recorded in phosphate buffered D_2O, pD 7.0, at concentrations of 0.1 mM, where all signals were essentially concentration independent. Resonances were assigned through a combination of COSY and NOESY spectroscopy.

Particularly dramatic were the changes in the aromatic region of the spectra of **1**−**10** (Figure 5), in which all signals moved upfield. The spectrum for the monomeric reference NDI **14** (Figure 5a) had a broad singlet at about 8.8 ppm corresponding to the aromatic protons, while this area in the spectra of many dimers contained two sets of signals, shifted upfield by as much as −0.5 ppm compared to **14**. For example, the aromatic NDI signals of **1** (Figure 5c) and **8** (Figure 5j) displayed a particularly large splitting of 70 and 100 Hz, respectively, while **3**−**5** (Figure 5e−g) exhibited little or no splitting. An intermediate splitting

(20) McMurray, J. S. *Tetrahedron Lett.* **1991**, *32*, 7679.

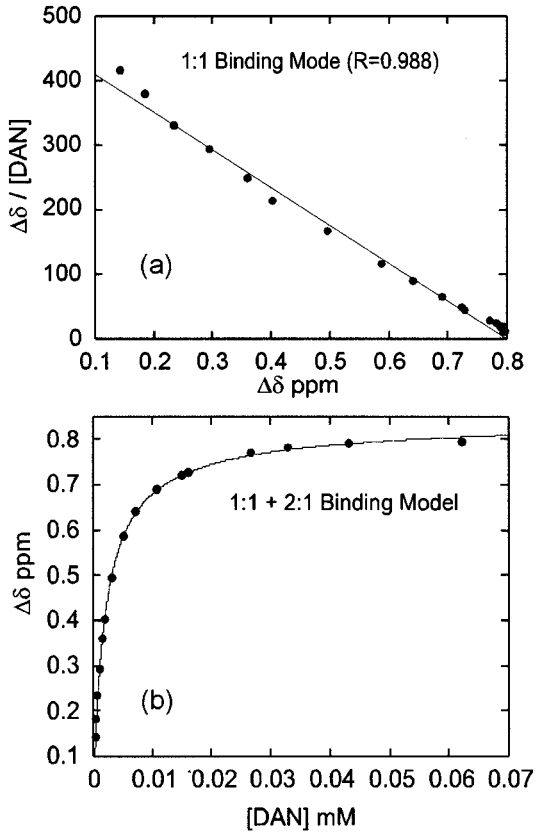

Figure 4. (a) Scatchard plot of NMR titration experiment with NDI **12** and DAN **13** monomers in D_2O. (b) NMR binding isotherm fit with a 1:1 + 1:2 binding model.

was observed for the remaining dimers. The aromatic NDI signals of **7** (Figure 5i) showed the greatest upfield shift of −0.5 ppm, while **9** (Figure 5k) showed the smallest change of about −0.3 ppm.

The monomeric reference DAN **15** exhibited two doublets (H-2, H-6 at 7.1 ppm and H-4, H-8 at 8.0 ppm) and one triplet (H-3, H-7 at 7.5 ppm), each integrating to two protons (Figure 5b). In many dimer compounds the equivalent pairs were split to give six total signals. This was especially prominent for **8** (Figure 5j) in which the $\Delta\delta$ between H-4 and H-8 is nearly 1.1 ppm and in **1** (Figure 5c), where the $\Delta\delta$ between H-2 and H-6 signals was greater than 0.7 ppm.

Significant changes were also observed for some linkage signals (Table 1). For example, ***k*** in **1** was shifted by about −0.7 ppm while ***j*** was shifted by less than −0.1 ppm compared to the reference compound **15**. Conversely, ***j*** was considerably more shifted in **9** than ***k***. Most of the other compounds exhibited small upfield shifts for ***j*** and ***k*** with little change in other linkage signals. An exception is **9** which displayed a $\Delta\delta$ of about −0.7 for ***c***. As expected for molecules containing a stereocenter and exhibiting folding, many diastereotopic methylene groups were observed, particularly in **9**.

Control compound **11** displayed a very broad, unresolved spectra at all concentrations examined, indicating extensive aggregation at room temperature. This behavior is in distinct contrast to the folding molecules **1**−**10**, which displayed well-resolved signals and chemical shifts essentially independent of concentration (below ∼1 mM) indicative of monomeric species. Higher temperature spectra of **11** were better resolved, but still suggestive of substantial aggregation, and thus not appropriate for comparison with **1**−**10**.

NOESY Spectroscopy. Weak intensity through-space couplings were observed between the NDI and DAN aromatic protons for all folding compounds except for **9**.[21] A portion of a typical spectrum is shown is Figure 6. Couplings were also observed between the linkage methylenes ***j*** and ***k*** with the NDI aromatic protons for all folding compounds except for **9**.[21] A number of other various long-range couplings were also observed for some compounds. A more detailed summary of the NOE data is available in the Supporting Information.

UV−Vis Spectroscopy. UV−vis data are summarized in Table 2. All 10 *folding* dimers showed significant absorbance spectral shape changes in the UV−vis region compared to a composite spectra derived from the superposition of isolated NDI **14** and DAN **15** monomer spectra. A representative example is shown in Figure 7. In particular, significant hypochromism was observed for each dimer in the 260−400 nm region. This hypochromism varied from 50% for **7** to 31% for **9** at 382 nm (see Table 2 for definition of % hypochromism). Importantly, the hypochromism was concentration independent in the range examined (<0.1 mM), indicative of monomeric species. Upon heating to 80 °C, the molar extinction coefficients at 382 nm (ϵ_{382}) increased by only about 4−6% for all folding dimers. In contrast, the control compound **11** showed hypochromism at room temperature analogous to compounds **1**−**10**; however, at 80 °C, *the ϵ_{382} of **11** increased dramatically*—over 40%.

A broad absorption band in the visible region, not observed in **14** or **15**, is observed for each of the folding dimers **1**−**10** (Table 2). The λ_{max} for these so-called "charge-transfer" bands was between 520 and 530 nm with the exception of **1**, which displayed a λ_{max} near 510 nm. The molar extinction coefficients for these bands at their respective λ_{max} range from 200 to 400 $M^{-1}\cdot cm^{-1}$ (Table 2).

Fluorescence. The DAN unit of **15**, which contains the same linkage as **2** but no NDI moiety, exhibited a strong, structured emission with a λ_{max} of 330 nm (Figure 8) and a 10 ps lifetime in aqueous phosphate buffer (pH ∼7). In contrast, shortened lifetimes, as well as substantial or complete quenching of this fluorescence, were observed for all dimers (Table 3). Where observable, the dimer steady-state emissions had a shape very similar to that of **15**. Interestingly, the entire emission for **9** was shifted with its λ_{max} observed at 308 nm compared to 330 nm for the other dimers.

Molecular Modeling. Unrestrained high-temperature molecular dynamics were used to produce a large set of random unfolded conformations for each dimer.[22] The unfolded structures were taken as a randomized set of starting structures that were then "folded" by annealing with a weak distance restraint between the NDI and the DAN units. The structures were then subjected to geometry optimization without any restraints.[23] Unfolded and distorted structures were discarded. This produced nine ensembles of structures with an energy range of about 5−10 kcal/mol (see the Supporting Information). In some instances (compounds **1**, **2**, and **6**), the collection consisted largely of structures with energies relatively close to that of the global minimum found for that compound. However, some of the collections, notably those for compounds **7** and **8**, showed a predominance of relatively higher energy structures.

(21) NOE spectroscopy was not performed on compounds **9** and **11** due to the degree of aggregation at concentrations where long-range NOEs could be observed.

(22) Compound **10** was excluded from the modeling studies since it has the same linkage as **2** and **11** was also excluded because it cannot physically fold in a manner analogous to **1**−**10**.

(23) It was not appropriate to derive distance restraints from the NOE data due to the poor quantitative value of these data as detailed in the "NOE Spectroscopy" portion of the discussion section.

Table 1. Chemical Shift Changes (ppm) for Dimers **1**−**10** Compared to NDI and DAN Reference Compounds **14** and **15**[a]

compound	*NDI linker signals*				*DAN linker signals*						*DAN aromatic signals*						*NDI aromtic signals*	
	b	***c***	***d***	***e***	***h***	***i***	***j***	***k***	***l***	***m***	**2**	**3**	**4**	**6**	**7**	**8**		
1	0.19	0.11	-0.19,-0.04	0.06	0.05	0.05	-0.07	-0.71	-0.24	-0.13	-0.31	-0.34	-0.82	-1.02	-0.60	-0.58	-0.26	-0.44
2	0.07	-0.12	-0.03,0.07	0.14,0.34	0.11	-0.15	-0.51,-0.42	-0.18	0.02	0.04	-0.67	-0.49	-0.62	-0.48	-0.60	-1.08	-0.28	-0.41
3	0.09	-0.06	-0.12,-0.05	0.07,0.14	-0.01	-0.12,-0.07	-0.32	-0.38	-0.09	-0.04	-0.64	-0.63	-0.99	-0.46	-0.42	-0.73	-0.28	-0.33
4	0.18	0.07	-0.06,-0.04	0.12	0.13	-0.03	-0.28	-0.34	-0.04	-0.02	-0.58	-0.53	-0.82	-0.67	-0.59	-0.86	-0.37	-0.40
5	0.17	0.03	-0.03,-0.01	0.17	0.14	0.00	-0.28	-0.33	-0.04	-0.01	-0.61	-0.62	-0.90	-0.61	-0.55	-0.85	-0.33	-0.37
6	0.09	-0.11	-0.05	0.18	-0.11	-0.26	-0.41	-0.27	-0.04	-0.03	-0.50	-0.46	-0.64	-0.56	-0.55	-0.88	-0.33	-0.41
7	0.17	0.04	-0.14	0.02	-0.18	-0.27,0.20	-0.55,-0.26	-0.25,-0.17	0.03	0.04	-0.61	-0.41	-0.59	-0.62	-0.68	-1.19	-0.37	-0.50
8	-0.08	-0.36	0.11	0.07,0.50	-0.26,0.33	-0.06	-0.15	-0.19	0.04	0.06	-0.36	-0.24	-0.39	-0.73	-0.99	-1.47	-0.14	-0.40
9	-0.27,-0.04	-0.86,-0.40	-0.16,0.12	0.07,0.36	-0.27	-0.52,-0.48	-0.92,-0.75	-0.18,-0.06	0.04	0.10,0.19	-0.84	-0.47	-0.51	-0.25	-0.34	-0.82	-0.18	-0.30
10	0.03	-0.22	-0.15,0.00	0.18,0.36	-0.12	-0.16	-0.58,-0.50	-0.08	0.22	-0.11	-0.66	-0.46	-0.63	-0.50	-0.67	-1.17	-0.27	-0.43

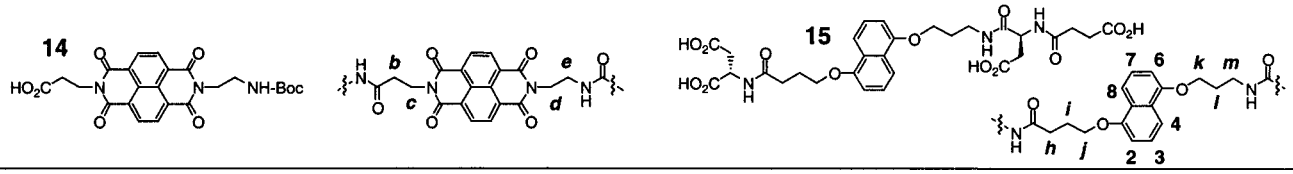

[a] Shifts were measured at concentrations of 0.1 mm in phosphate-buffered D_2O. At these concentrations the shifts were essentially concentration independent. Entries with two values represent diastereotopic proton pairs.

For the purposes of this analysis, attention was focused especially on the relative orientations of the aromatic units, since the NMR analysis is based on these regions of the molecules. Structures were defined as "folded" if the centers of the DAN and NDI ring planes were within ~5 Å of one another and the angle between the planes was less than 30°. A coordinate system was defined with its origin at the center of the NDI unit (Figure 9a). By setting a reference point at the center of the DAN unit, the relative orientation of the DAN/NDI complex can be described with three parameters: *x offset*, *y offset*, and *DAN/NDI axis angle* (Figure 9). The DAN/NDI axis angle, α, is defined as shown in Figure 9b. The distribution of each parameter for each linkage is shown in Figure 10.

The types of orientations produced during the simulations vary significantly between different linkages in some instances. Notably, the dimer with the shortest linkage **1**, displays the most limited range of NDI/DAN orientations. Most of structures generated with this linkage exhibit significant *x* offset of the DAN unit away from the linkage side of the diimide. Also, the range of α angles produced with this linkage is rather limited. In contrast, a general trend toward greater orientation diversity is seen with increasing linker length. For example, the dimer with the longest linkage, **5**, shows the widest array of offsets and α values. The overall scatter of x offsets also becomes more centered about the central reference point of the NDI with increasing linker length. Some linkages show a weak partitioning of lower and higher energy structures, defined as within or above 5 kcal/mol of the minimum respectively, along the *x* axis. This partitioning is most pronounced in **7** and **8**. For **8** and to a lesser extent **7**, *all* the low energy structures had a negative *x* offset (left of the origin in Figure 9a, away from the linkage side of the NDI) and the majority of low energy structures had a major *x* offset.

Chemical Shift Simulation. An algorithm was developed to simulate the chemical shift changes caused by the anisotropy of the NDI and DAN units. Briefly, these calculations derive predicted chemical shift changes from the distance and angle between a particular proton and the shielding entities. An empirical function was used to approximate the shielding/deshielding effects of the aromatic rings[24a] while a separate function was used for the carbonyls of the NDI unit.[24b] Details of the calculations are discussed in the Experimental Section. Shift changes were calculated for twelve protons, or sets of equivalent protons, common to all dimers (values for diastereotopic proton pairs were averaged). Thus, the simulated chemical shift changes for any individual structure, *or combination of structures*, obtained from molecular dynamics could be calculated and compared to the observed shift changes.

Single structures showed a wide range of agreement with observed data (see the Supporting Information). Quality of fit was quantified by the root-mean-square (rms) difference between observed and calculated shift changes. In the case of **1,** there was a rough correlation between the rms fit and potential energy. In no instance did the lowest energy structure found also have the smallest rms difference. However, in many instances there were relatively low energy structures with reasonably good rms fits (>0.2 ppm).

Discussion

Monomer Studies. To obtain reliable parameters for complex formation, a significant portion of the binding curve must be obtained from a titration experiment.[25] Previous binding titrations using derivatives of NDI and DAN were hindered by limited solubility in aqueous solvent and/or complications due to the use of like-charged molecules.[14a] The increased solubility of the neutral monomers, **12** and **13**, allowed for near saturation as seen in the binding isotherm shown in Figure 4b. A Scatchard plot (Figure 4a) of the NMR titration data exhibited significant curvature. Curved Scatchard plots are consistent with 2:1 or higher order complex formation concurrent with 1:1 complex-

(24) (a) Abraham, R. J.; Fell, S. C. M.; Smith, K. M. *Org. Magn. Reson.* **1977**, *9*, 367. (b) Herranz, J.; Gonzalez, C.; Rico, M.; Nieto, J. L.; Santoro, J.; Jimenez, M.; Bruix, M.; Neira, J. L.; Blanco, F. J. *Magn. Reson. Chem.* **1992** *30*, 1012.

(25) Deranleau, D. A.; *J. Am. Chem. Soc.* **1969**, *91*, 4044.

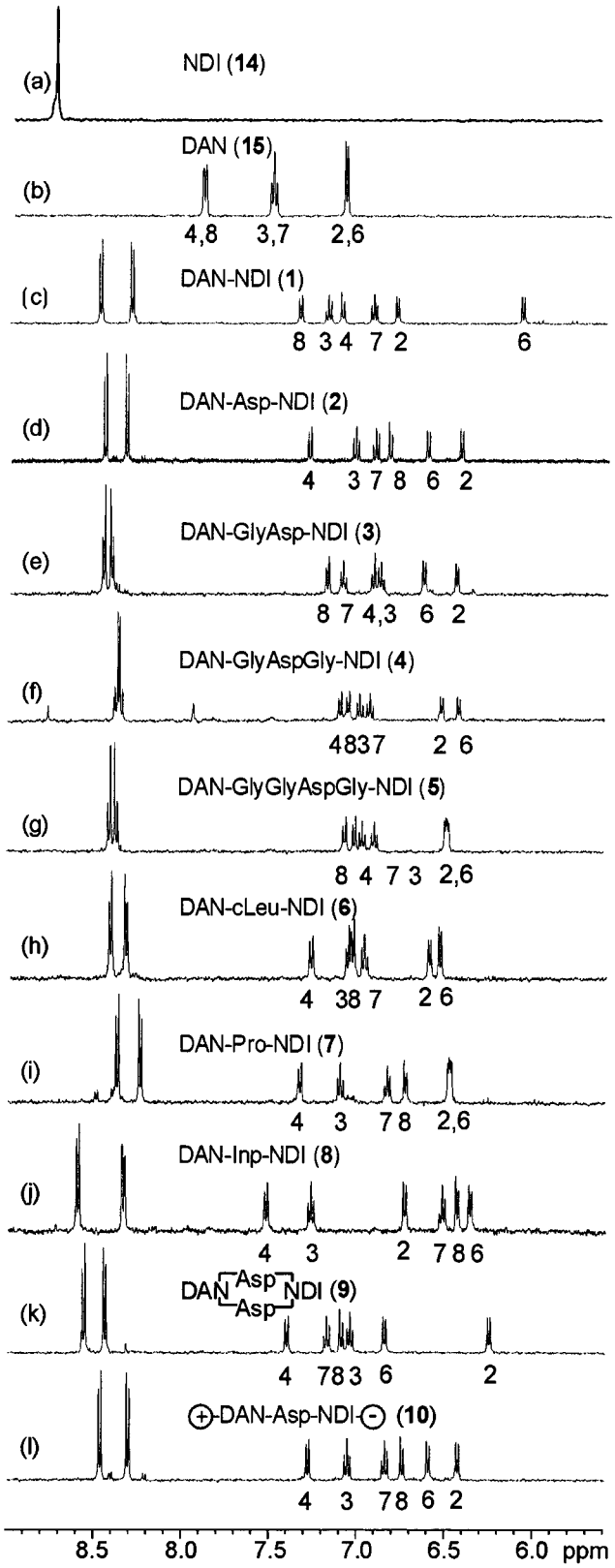

Figure 5. Aromatic region of 500 MHz ^{1}H NMR of compounds **1**−**10**, (c)−(l) respectively, in phosphate buffered D_2O at a concentration of 0.1 mM. Also shown, monomeric reference compounds NDI **14** and DAN **15**, (a)−(b) respectively, at 0.1 mM in buffered D_2O.

ation.[26] Note that the Scatchard plot is much more sensitive to the possible presence of higher order complexes than the Benesi−Hildebrand plot and should be used whenever there is a possibility of multiple equilibrium.[17a]

Due to the curvature observed in the Scatchard plot (Figure 4a), a model presuming both 1:1 and 2:1 binding was used to fit the NMR titration data[27] (Figure 4b). Fitting experimental data to multiple parameters has significant inherent error. Nevertheless, the derived values provide a reasonable estimate

(26) Note that higher level complexation is not confirmed or ruled out by the observed Scatchard plot curvature, but is merely consistent with such observations.

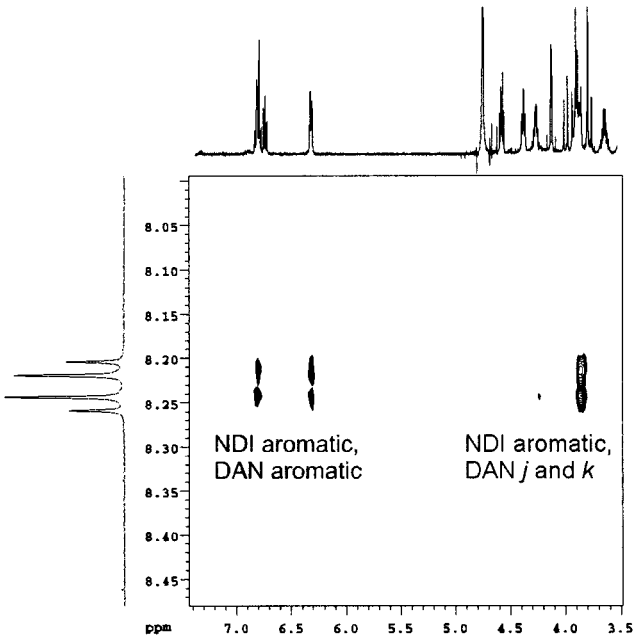

Figure 6. Portion of NOESY spectrum for dimer **5** showing long-range couplings between NDI aromatic protons with DAN aromatic protons and linkage methylenes ***j*** and ***k***.

Table 2. Summary of UV−Vis Data for Dimers **1**−**10**

compd	% hypochromism at 382 nm[a,b]	charge transfer (CT) λ_{max}	molar extinction coefficient[c] at CT λ_{max}
1	38	510	410
2	45	526	330
3	39	526	260
4	43	520	360
5	49	520	370
6	43	528	260
7	50	526	390
8	49	526	180
9	31	526	210
10	40	526	340

[a] % hypochromism = [1 − (molar extinction coefficient of dimer/molar extinction coefficient of **14**)] × 100%. $\epsilon_{14} = 26\,600$. [b] Measured at concentrations of ∼30 μM or below. [c] $M^{-1}\cdot cm^{-1}$.

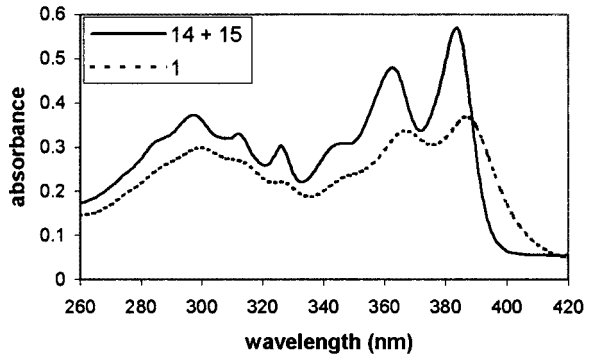

Figure 7. UV spectra of dimer **1** compared to a composite spectra of NDI **14** and DAN **15** reference compounds. Concentrations are 20 μM in phosphate-buffered H_2O. Molar extinction coefficients were concentration independent at these concentrations.

Table 3. Summary of Fluorescence Data for Dimers **1**−**10**

compd	rel quantum yield[a]	lifetime (ps)
15	1.00	10.0
1	0.02	7.2
2	0.02	7.5
3	0.01	6.7
4	0.10	9.7
5	0.09	9.4
6	0.00	4.6
7	0.00	3.4
8	0.00	5.4
9	∼0.1[b]	6.5
10	0.00	4.7

[a] Excitation $\lambda = 296$ nm. [b] Estimated due to difference in emission λ_{max}; **15** −330 nm, **10** −310 nm.

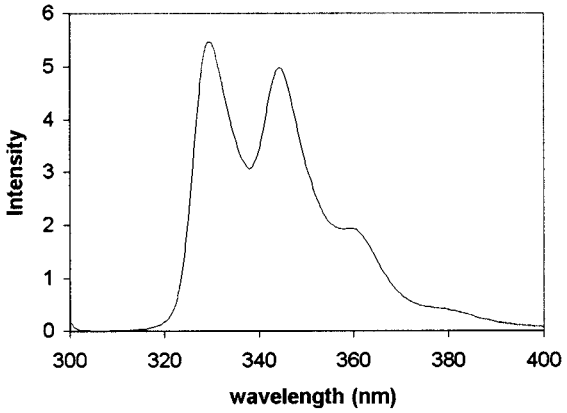

Figure 8. Emission spectra of DAN reference compound **15** at a concentration of 2.0 μM in phosphate buffered H_2O.

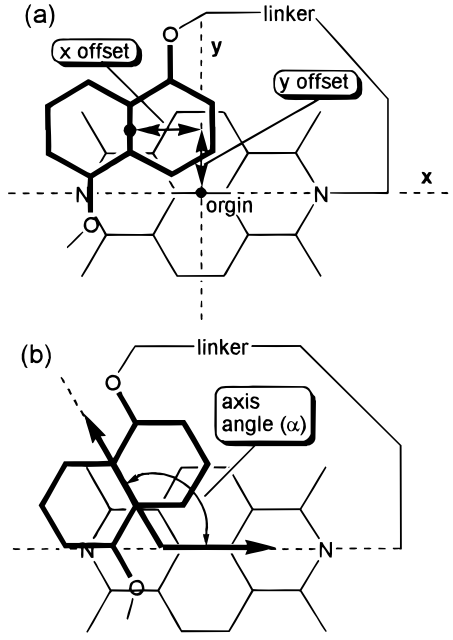

Figure 9. Coordinate system and orientation parameters for NDI/DAN interaction. (a) x and y offset. (b) NDI/DAN axis angle α.

of the association constants and chemical shift changes for NDI/DAN complexes in water. Significantly, the *upfield* shifts of the NDI aromatic protons observed in titrations of **12** and **13** are consistent with *face-to-face*, or parallel, complexation, as proposed for the dimer molecules.[28] The magnitude of the NDI aromatic proton $\Delta\delta$ derived for a 1:1 DAN/NDI complex (−0.42 ± 0.10 ppm) is comparable to those observed for the dimer compounds (−0.3 to −0.5 ppm) **1**−**10**.[30] Thus, it can be proposed that NDI and DAN have a substantial face-to-face interaction in aqueous solution, leading to the prediction that the dimer molecules will adopt relatively stably folded, compact structures in water.

^{1}H NMR Chemical Shift Changes. The chemical shift changes observed in all 10 folding dimers are entirely consistent with face-to-face association of the NDI and DAN units. All $\Delta\delta$ for the DAN and NDI aromatic signals are *upfield* [28] compared to the reference compounds **14** and **15** (Table 1). The observed chemical shifts, therefore, argue against significant contributions from conformations with edge-to-face association of the NDI and DAN units.

Chemical shift changes can contain significant conformational information and have been previously employed in this manner.[11a,31] The aedamer system is particularly well suited to such an approach due to the strong anisotropy of the aromatic units and their close proximity to one another in folded structures. Shift calculations give considerable insight into how different NDI/DAN geometries can affect the chemical shifts and splitting patterns of the aromatic region of aedamer NMR spectra. Unlike NOESY spectroscopy, chemical shifts can easily be obtained even at very low sample concentrations. This is advantageous when self-association at higher concentrations is a significant problem.

The change of the NDI aromatic signal from a broad singlet, as in the reference compound **14**, to an apparent AA′BB′ pattern (two distorted "doublets") in many of the dimers (Figure 5c−l) is attributed to differential shielding along the NDI *x* axis caused by DAN complexation (Figure 11). Each "doublet" is assigned as a pair of protons, A and A′ for example, made equivalent due to fast rotation of the NDI unit about the *x* axis.[32] Four different signals would be expected if fast rotation on the NMR time scale was not occurring, unless the average complex was very nearly symmetrical about either the x or y axes. Since four different signals were not observed for *any* of the 10 folding dimers, fast rotation, as opposed to all symmetrical complexes, is the more plausible explanation for the AA′BB′ pattern.

The chemical shift difference between AA′ and BB′ can be interpreted as an indication of the average offset along the *x* axis of the DAN/NDI coordinate system (Figure 9). A significant shift difference between AA′ and BB′ signals of the NDI residues is consistent with the DAN being substantially offset from the origin along the *x* axis (Figure 11a). Conversely, a small or absent shift difference is consistent with the average DAN position being more centered around the origin (Figure 11b) of the NDI. In line with expectation, dimers with the

(27) Higher order complexation, beyond 2:1, cannot be rigorously ruled out. However, the assumption of a 2:1 + 1:1 binding model seems reasonable where the concentration of one component is in considerable excess through most of the titration.

(28) Upfield chemical shifts are experienced in the regions of space directly above aromatic and carbonyl pi systems while downfield shifts are experienced in the plane of the π system.[29]

(29) Gunther, H. *NMR Spectroscopy*, 2nd ed.; John Wiley & Sons: New York, 1995; 78−93.

(30) It is not appropriate to quantitatively compare the $\Delta\delta$ values derived for the complex with those for dimers **1**−**10** since the geometry of the *intramolecular* dimer complex may vary significantly from that of the *intermolecular* monomer complex.

(31) (a) Hunter, C. A.; Packer, M. *Chem. Eur. J.* **1999**, *5* 1892. (b) Schneider, H.-J.; Rudiger, V.; Cuber, U. *J. Org. Chem.* **1995**, *60*, 996. (c) Schneider, H.-J. *Recl. Trav. Chim. Pays-Bas* **1993**, *112*, 412. (d) Abraham, R. J.; Rowan, A. E.; Mansfield, K. E.; Smith, K. M. *J. Chem. Soc., Perkin Trans. 2* **1991**, 515. (e) Tachiyashiki, S.; Yamater, H. *J. Chem Soc. Dalton Trans.* **1990**, 13. (f) Fukazawa, Y.; Ogata, K.; Usui, S. *J. Chem. Soc.* **1988**, 110, 8692.

(32) Note that it is not possible to assign which of the two "doublets" is actually AA′ or BB′.

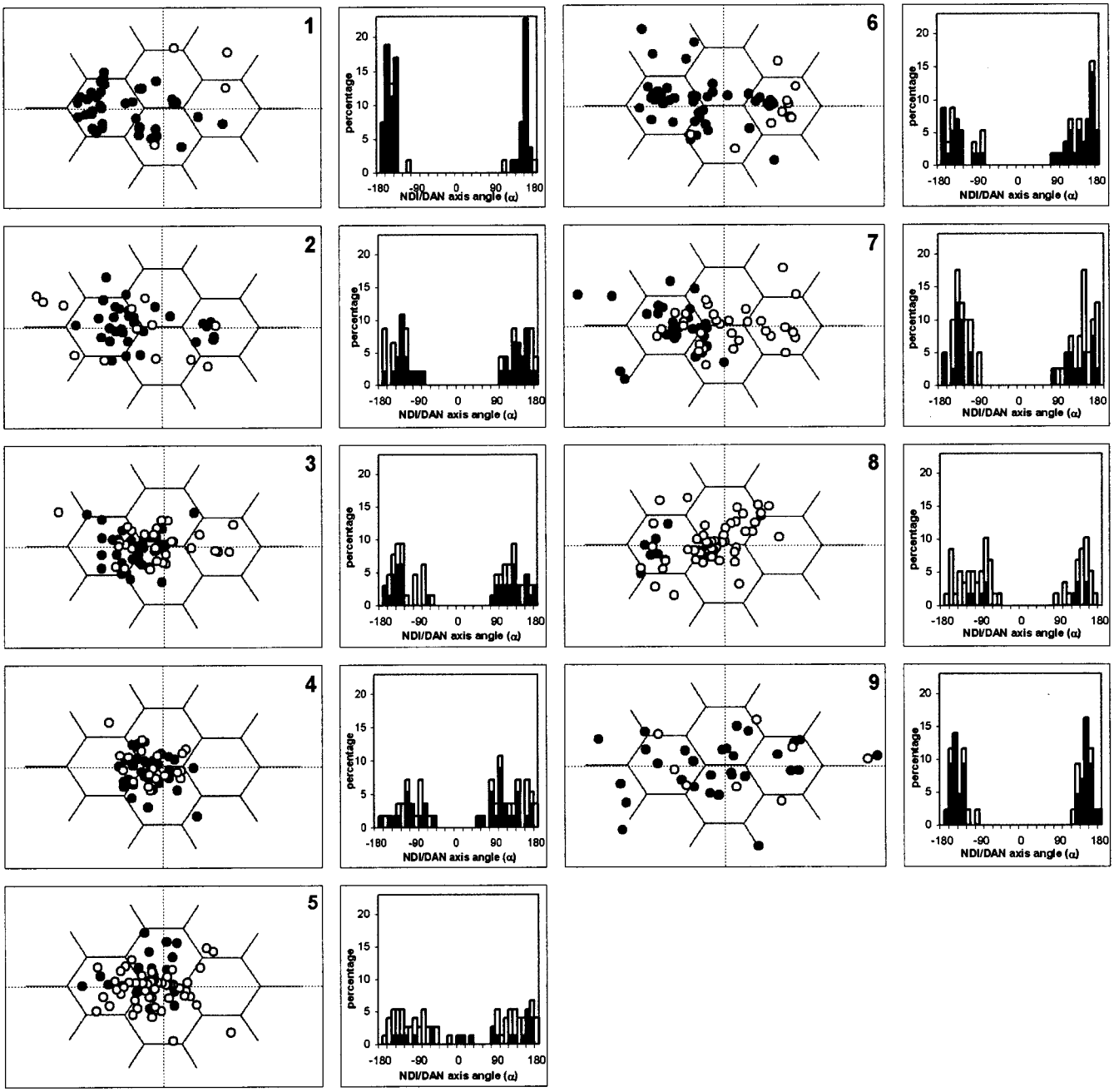

Figure 10. Distribution of NDI/DAN orientation parameters for molecular modeling ensembles of dimers **1**−**9**. Left panels: *x* and *y offset*, each circle represents the center of the DAN unit. Right panel: *NDI/DAN axis angle* α. Filled circles and bars represent structures within 5 kcal/mol of the lowest energy conformer found for that compound. Open circles and bars represent structures with energies 5 kcal/mol or more above the lowest energy conformer. The linkage is attached to the right side of the NDI outline. See Figure 9 for definition of orientation parameters.

longest linkers such as **3**−**5** (Figure 5e−g) have NDI signals consistent with nearly centered DAN complexation while the dimers with shorter and/or more rigid linkers, such as **1** and **8**, display spectra consistent with a large offset (Figure 5c,j).

The splitting of DAN signals is correspondingly influenced by the stacking orientation in the dimers. For the monomeric species, three pairs of equivalent protons are observed, even when the alkoxy groups are different as in **15** (Figure 5b). However, unsymmetrical complexation in the dimers produces significant splittings. For example, H-6 (Figure 5c) of **1** is shifted by about −1.0 ppm, while H-2 is only shifted by −0.3 ppm compared to the same signals in **15**. The large upfield shift experienced by H-6 indicates that, in a significant number of important conformers, this proton must be near the strong shielding zone of the NDI naphthalene core while H-2 must be

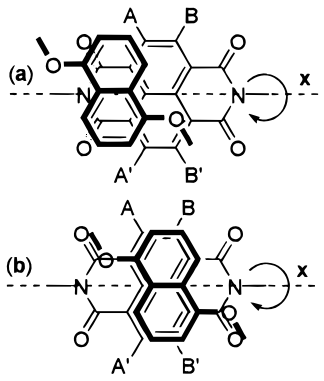

Figure 11. Schematic representation of DAN offset relative to NDI. (a) "Large" x offset. (b) "Small" x offset.

considerably more remote. A similar, but more dramatic example is the difference between H-4 and H-8 in compound **8** (Figure 5j). Here, H-4 is shifted by −0.4 ppm while H-8 is shifted by nearly −1.5 ppm, suggesting that in a significant number of conformers, H-8 must be directly above the shielding zone of the NDI naphthalene core. Dimers **2** and **6**−**10** also exhibit major splitting in one or more of their DAN proton pairs consistent with significant stacking asymmetry. As with the NDI aromatic signals, dimers with longer linkages, **3**−**5** display little splitting indicating a higher degree of symmetry in the intramolecular NDI/DAN complex.

The chemical shifts of the linker methylene groups also provide an indication of NDI/DAN orientation. For example, in compound **1**, ***k*** is shifted by −0.7 ppm while ***j*** is shifted by only about −0.1 ppm relative to the same signals in the reference compound **15**. This large difference is consistent with ***k*** being much closer to the shielding zone of the NDI compared with ***j*** in a significant number of important conformers. Note that this is consistent with the $\Delta\delta$ difference between DAN H-2 and H-6 since H-2 is adjacent to ***j*** and H-6 is adjacent to ***k***. Interestingly, the reverse order of $\Delta\delta$ magnitude is observed for dimer **9**, suggesting that ***j*** and DAN H-2 must be closer in this case.

NOESY Spectroscopy. The observed long-range couplings are consistent with all 10 of the folding dimers existing in a compact, folded state. In particular, numerous cross-peaks were observed for all of the folding dimers between the aromatic NDI protons and the DAN aliphatic as well as aromatic protons. In addition, the patterns of cross-peaks was somewhat different for the different compounds. As with the other spectroscopic data, the most straightforward interpretation of these findings leads to a face-to-face folding model.

Unfortunately, there are several factors that prevent an unambiguous structure assignment for the different dimers based solely on a *quantitative analysis* of the observed NOE data. First, the molecular modeling, as discussed in more detail below, suggests that numerous nearly isoenergetic conformational states may be available to some compounds. Thus, any observed coupling may actually be the average of several couplings in significantly varying conformations. In addition, the equivalence of the NDI aromatic AA′ and BB′ protons, caused by rotation of the NDI around the *x* axis complicates much of the detailed distance information contained in any thru space couplings with these protons (Figure 11). Finally, concentrations must be kept relatively low to avoid significant self-association, thus increasing signal/noise ratio problems. Note that having to use low concentrations also introduced the complication of longer mixing times, resulting in spin-diffusion concerns.

The NOEs listed are *qualitatively* useful, however, in evaluating any potential structures or ensemble of structures derived from the predicted/observed ^{1}H NMR chemical shifts. In other words, if a proposed structure or ensemble of structures predicts a particular strong NOE, it should be observable. Conversely, there should not be an observed NOE that is not predicted by a proposed structure or ensemble of structures.

UV−**Vis Spectroscopy**. Significant UV hypochromism, compared to the isolated NDI and DAN moieties in **14** and **15**, respectively, is observed for all of the dimers (Table 2), again, entirely consistent with face-to-face NDI/DAN complexation[14a] in the folded dimers. In theory, subtle variations in the observed degree of hypochromism could reflect differences in either the amount of complex present or the geometry of the complexes. Very little change is seen in this hypochromism over the range of 25−80 °C with any of the folding dimers **1**−**10**. Assuming a two state model, a large temperature increase would be expected to help favor the unfolded state if the two states *have similar free energies*. The lack of temperature dependence therefore suggests that the folded/unfolded equilibrium strongly favors the folded state.

Charge-transfer (CT) bands are also observed for all folding dimers consistent with NDI/DAN complexation[14a] (Table 2). The CT λ_{max} varies slightly among almost all of the different dimers, implicating some variation in the relative NDI/DAN geometry, since orbital interactions are dependent on orientation. Only **1** exhibits a significantly different CT λ_{max} of about 510 nm suggestive of a unique NDI/DAN geometry. This could be correlated with the relatively limited, and unique, NDI/DAN α angles available with this linkage as predicted by molecular mechanics (Figure 10).

The control compound **11** shows hypochromism at room temperature, but at 80° C, the hypochromism decreases dramatically. This degree of temperature dependence was not observed with any of the folding dimers, **1**−**10**. In addition, compound **11** was the only molecule exhibiting a very broadened NMR spectra indicating extreme aggregation. The temperature dependent change in hypochromism can be explained with the reasonable assumption that *inter*molecular aromatic−aromatic interactions are more easily disrupted at higher temperature for entropic reasons compared to the *intra*molecular interactions of the folding systems **1**−**10**. In this way, compound **11** serves as an important control that illustrates behavior expected if any of the folding dimers did not exist primarily in the proposed folded, compact conformations in solution. Thus, such a dramatic change in behavior for **1**−**10** vs **11** can be viewed as further evidence that **1**−**10** exist in largely and/or completely folded states in solution.

Fluorescence. If energy transfer mechanisms are ignored, the extensive quenching of DAN fluorescence observed for all dimers is also consistent with a predominance of folded conformations in aqueous solution. The very weak (essentially not observable in steady-state experiments) luminescence in compounds **6**−**8**, **10** is attributed to nearly complete complexation of the NDI and DAN units. Complexed DAN is not expected to exhibit luminescence since CT complexes have low energy states available for very fast nonradiative decay.[33,34] Quenching can occur by excitation of a preformed complex (static quenching), by NDI complexation of an excited DAN (dynamic quenching) or a combination of the two. If only dynamic quenching is occurring, then the relationship $I/I_o = \tau/\tau_o$ should hold true where I is the emission intensity of the DAN in the presence of NDI, I_o is the emission intensity of the DAN in the absence of NDI, τ is the emission lifetime of the DAN in the presence of NDI, and τ_o is the emission lifetime of the DAN in the absence of NDI.[35] Since $I/I_o >>> \tau/\tau_o$ is observed, most of the quenching is attributed to complexed DAN. Thus, even dimers exhibiting lifetimes similar to **15** and measurable steady state emission intensities are likely to exist in a predominantly complexed state.

Unfortunately, any quantitative analysis of the quenching data is precluded by the complicating possibility of a third quenching mechanism, resonance energy transfer. There is significant overlap of the DAN emission with the NDI absorption.

(33) Ashton, P. R.; Ballardini, R.; Balzani, V.; Boyd, S. E.; Credi, A.; Gandolfi, M. T.; Gomez-Lopez, M.; Iqbal, S.; Philip, D.; Preece, J. A.; Prodi, L.; Ricketts, H. G.; Stoddart, J. F.; Tolley, M. S.; Venturi, M.; White, A. J. P.; Williams, D. J. *Chem. Eur. J.* **1997**, *3*, 152.

(34) Such quenching would be unresolvably fast in this experiment where resolution was on the order of 50 ps.

(35) MacKenzie, R. E.; Fory, W.; McCormick, D. B. *Biochemistry* **1969**, *8*, 1839.

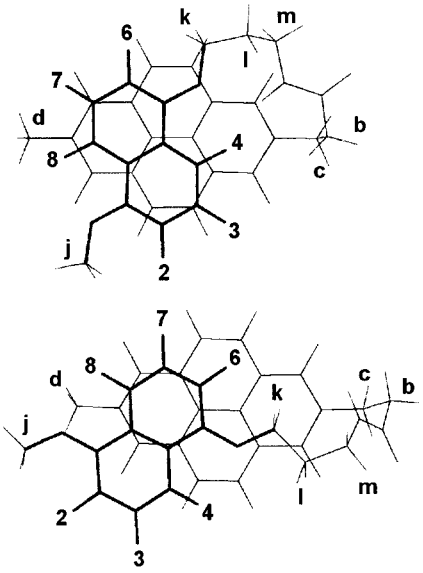

Figure 12. Low energy conformations of dimer **1** that, in combination, provide a good fit with the observed spectroscopic features.

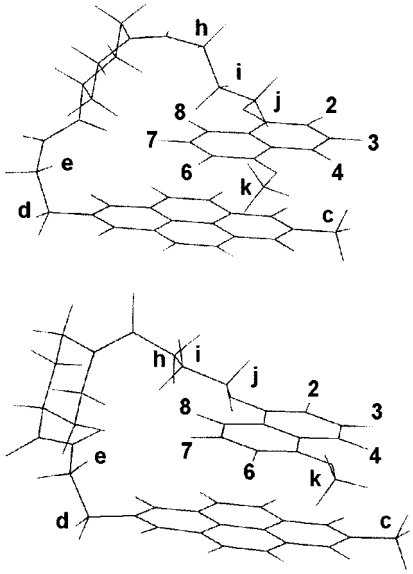

Figure 13. Low energy conformations of dimer **8** that, in combination, provide a good fit with the observed spectroscopic features.

Additionally, dimers with the shortest and most rigid linkers display the greatest degree of quenching, perhaps consistent with energy transfer playing a dominant role in these systems. However, note that dimer **6**, which has the same linkage length as **2** but is presumably more rigid, exhibits almost no detectable emission in contrast to **2**. The identical linkage lengths should nearly equalize resonance energy transfer effects between the two compounds suggesting that the observed complete quenching in the more rigid dimer indicates a slightly greater degree of complexation. Dimer **10** also has the same linkage length as **2** and presumably the same approximate magnitude of resonance energy transfer effects. Nevertheless, **10** displays no detectable emission, unlike **2**. This could be interpreted as a greater degree of complexation compared to **10** due to the formation of an intramolecular salt-bridge. The red-shift in the emission of **9** compared to all other dimers is likely attributed to fewer nonradiative decay mechanisms available to the rigidified cyclic structure.

Detailed Analysis of Individual Dimers. By combining the predicted information from the molecular modeling and chemical shift calculations with the experimentally observed spectroscopic data, a number of conclusions could be reached regarding the detailed conformations of the different dimers. In each case, attempts were made to fit (1) one or more low energy structures, (2) selected groups of structures, or (3) the entire ensemble of predicted structures to the observed spectroscopic data. NOE data were useful as a qualitative tool to help make decisions about the feasibility of structural predictions.

Compound 1. A combination of the two structures in Figure 12 or the entire conformational collection predict the observed spectra equally well. It is interesting to note that the two structures in Figure 12 correspond, in terms of the *x* offset, with the two major "clusters" seen in the entire conformation collection (Figure 10). Thus, considering only the two structures may be a simplified way to view the entire ensemble. Overall, the observed spectra is consistent with significant asymmetry in the NDI/DAN complex and *x* offset (note the relatively large difference in delta shift for AA′ versus BB′) of the DAN unit away from the linkage side of the NDI. A large *x* offset and limited number of NDI/DAN axis angles might explain the observed altered CT λ_{max} (510 nm).

Compound 2. The entire collection of conformations gives a better match with the observed data than any single low energy structure or combination of such conformers. The NDI/DAN complex is rather asymmetric as seen by many differential shift changes. However, the difference between AA′ and BB′ is significantly less than that observed for **1**, suggesting that the x offset is somewhat diminished. This trend is also seen in the conformational mapping (Figure 10).

Compounds 3−5. Averaging over the entire conformational collection gave a good fit to the observed data in each case. Here, a clear trend toward greater symmetry in the NDI/DAN complex with increasing linkage length (Figure 5e−g) was observed. This structural interpretation of the data is consistent with the intuitive notion that dimers with the more flexible linkers should be thought of as extremely dynamic structures in which aromatic stacking is maximized in the time-averaged structure.

Compound 6. Again, the averaged collection best satisfies the observed data. **6** displays a shift pattern generally similar to **2**, and the calculated structures, as evidenced by the NDI/DAN orientation parameters, are similar as well between these two compounds. The most significant spectral difference between **6** and **2** is that both the predicted and observed spectra suggest a slightly more symmetrical complex of **6** compared to **2**, manifested in a smaller AA′ vs BB′ difference and near overlap of DAN H-3 and H-8. Compound **6** has the same linkage as **2** with the exception of the ring system on the amino acid residue α carbon of **6**. Thus, it is interesting that the incorporation of the presumably rigidifying cyclopentane unit seems to have only minor effects on the conformation of the system.

Compound 7. The averaged ensemble of structures again gave the best match with the observed data. Overall, the degree of asymmetry and *x* offset are on the order of that observed for **2** or **6**.

Compound 8. In this instance a 1:1 combination of two low energy conformers provides the best prediction of the observed data (Figure 13). Note that both types of conformers have the cyclic linkage element in a presumably low energy chair conformation and that the average *x* offset of the two is substantial, in agreement with the very large shift difference seen between AA′ and BB′.

Compound 9. The lack of observable long-range through-space couplings, at concentrations where aggregation is minimal, hinders the analysis of this structure. However, chemical shift changes can still provide considerable information about major structural features. Interestingly, the aromatic region of **9** closely resembles that of **1**, except for the reversal of order for former equivalent pairs (in descending ppm: dimer **1**; H-8, H-3, H-4, H-7, H-2, H-6, dimer **9**; H-4, H-7, H-8, H-3, H-6, H-2). Also, both compounds show major shift changes for the $O-CH_2-CH_2-$ methylenes of the DAN unit. However, for **1** signals, ***k*** and ***l*** are shifted downfield, while for **9** it is ***j*** and ***i*** that are most affected. All of this suggests a significantly offset structure, but in the opposite direction as that proposed for **1**. This may seem surprising since both linkages of **9** are of equal length and constitution compared with **1**. However, they do have the opposite N to C directionality, which apparently must account for the observed asymmetry. Single structures, combinations, and the entire ensemble all gave a poor reproduction of the observed data. The reasons for this failure are unclear. It is possible that the "folded" conformational space of this compound was not adequately sampled due to its rigid, restrained nature. Alternatively, the particular conformations of this compound may fortuitously exaggerate inaccuracies in the functions used to simulate the shift changes.

Compound 10. A conformational analysis was not carried out for this compound since it has the same linkage as dimer **2**. Nonetheless, it is interesting to examine its spectra compared to compound **2** (Figure 5d,l). Compound **10** was synthesized with a free N-terminus to allow for the possibility of noncovalent cyclization thru salt-bridge formation. No direct evidence of such cyclization was observed. The compounds exhibited very similar NMR and UV spectra. There was some difference in the observed fluorescence; **10** displayed essentially complete quenching in steady-state experiments, while **2** showed a small residual emission. Also, **10** had a significantly shortened fluorescence lifetime compared to **2**. All this suggests that **10** has a distribution of conformers very similar to **2** in solution, but may have an equilibrium that favors folded states to a somewhat greater extent.

Conclusions

All 10 of the *folding* dimers, **1**−**10**, exhibited spectroscopic properties fully consistent with a predominance of folded structures in solution, although the exact orientation of the NDI/DAN complex was linkage dependent. A simple interpretation of observed spectra did not lead to realistic structural prediction. Rather, molecular modeling, including chemical shift simulation, combined with the spectroscopy provided an approach to characterizing solution structure. In most instances, the observed data were best explained by a large ensemble of structures as opposed to one or few conformers. Thus, in the case of these aedamer dimers, "folding" does not appear to imply a two-state model with a rigid, uniquely folded structure, but rather a dynamic situation in which the molecule spends the majority of its time in different folded conformations. These folded conformations are far from random for a given molecule, however, in that they share the key structural feature of having the aromatic units stacked in a face-to-face orientation.

The robustness of the aromatic stacking motif in water has been demonstrated by extensive modification of the aedamer linkage without disruption of the overall folded structure. Such behavior in aqueous solution is particularly significant since it will allow for consideration of interactions with biological systems. In general, longer linkages allowed for more symmetrical face-to-face aromatic stacking, while shorter or more rigid linkages caused greater asymmetry/offset of the stacked complex. The equilibrium between unfolded/folded states may be driven toward folding by more rigid linkages, but even the longest and most flexible linkages apparently produced a clear predominance of folded conformations based on all of the spectroscopic data. This latter point was emphasized by the observed high level of aggregation and unique temperature-dependent spectra of the control compound **11**, a molecule that is geometrically prevented from folding. Any of the dimers (**1**−**10**) in the study that were not predominantly folded in solution would have been expected to mimic more the observed behavior of **11**.

The characterization of solution conformation represents a key element of foldamer research. The preceding analysis has demonstrated that the powerful spectroscopic handles associated with the stacking of aromatic units in folded aedamers can be exploited to obtain a dynamic, working model of folded structure in aqueous solution. The analysis described in this study can therefore be considered a blueprint for the design and structural characterization of more elaborate, and ultimately functional, aedamers and related foldamers.

Experimental Section

General Methods. Commercially available reagents and solvents were used without further purification unless noted otherwise. DMA and DMF for peptide couplings were stored under dry argon with 4 Å molecular sieves. Organic solvent solutions were dried over Na_2SO_4 and evaporated on a rotary evaporator under reduced pressure. Flash chromatography was performed using 230−400 mesh silica gel. All aqueous solutions were prepared in 50 mM sodium phosphate buffer (pH ∼7).

Spectroscopy. (NMR) Routine 1-D spectra were recorded on a Varian UNITY+ 300s. All other spectra were recorded on a Varian INOVA 500. Chemical shifts are reported in ppm relative to tetramethylsilane (TMS) for organic solvents and relative to $(CH_3)_3SiCD_2CD_2CO_2Na$ (TSP) in aqueous solution. Mixing times for NOE experiments were 500 milliseconds. Concentrations for NOE experiments were kept between 1.5 and 2.0 mM. UV−vis spectra were recorded on a Hewlett-Packard 8452A diode array spectrophotometer. Steady-state fluorescence measurements were performed on a Perkin-Elmer LS50 spectrofluorimeter. Emission intensities were corrected for differences in absorbance at the excitation wavelength (296 nm) to give relative quantum yields. Fluorescence lifetimes were measured by time-correlated single-photon counting using a mode-locked, synchronously pumped, cavity-dumped dye laser. The excitation wavelength used was 296 nm while the emission was monitored at a variety of wavelengths between 320 and 420 nm. Decay profiles were fit to a single exponential.

NMR Titrations. 16 D_2O solutions were prepared with **12** kept at a constant concentration of 0.20 mM and **13** varying from 0.60 mM to 62.27 mM. The $\Delta\delta$ of the aromatic protons of **12** was calculated by subtracting from the δ of **12** only at 0.20 mM (8.75 ppm). For the assumption of concurrent 1:1 and 2:1 complexation the binding isotherm was fit to eq 1[18]

$$\Delta\delta = \frac{K_1\Delta\delta_1[\mathbf{13}]_o + K_1K_2\Delta\delta_2[\mathbf{13}]_o^2}{1 + K_1[\mathbf{13}]_o + K_1K_2[\mathbf{13}]_o^2} \qquad (1)$$

where K_1 is the equilibrium constant for the formation of **12**−**13**, K_2 is the equilibrium constant for the formation of **13**−**12**−**13**, $\Delta\delta_1$ is the shift of the **12**−**13** complex, $\Delta\delta_2$ is the shift of the **13**−**12**−**13** complex, and $[\mathbf{13}]_o$ is the total concentration of **13**. The data were fit using Kaleidagraph 3.0.5[36] with the restraint $\Delta\delta_2 = 2\Delta\delta_1$.

(36) Synergy Software, 1994, 2457 Perkiomen Ave, Reading, PA 19606.

Molecular Modeling. All modeling was performed in HyperChem[37] using the MM+ force field. Programming was developed in Excel[38] 4.0 Macro Language to automate annealing/optimatization operations in HyperChem and to return data (atomic coordinates, energies, etc.) to Excel spreadsheets for calculations. Structures were truncated after methylenes ***k*** and ***c*** (***j*** and ***d*** for compound **1**) to make the calculations more expedient. *Conformer collections*: For each dimer examined, 10 random starting structures were each subjected to 10 ps of unrestrained molecular dynamics at 1000 K with snapshots taken every ps to give 100 structures for annealing. A weak distance restraint was then applied between the centers of the NDI and DAN units while the simulation temperature was lowered to 300 K over 5 ps. The structures were then refined by unrestrained geometry optimization (Fletcher−Reeves conjugate gradient, 0.01 kcal/mol). *Chemical shift simulation*: The chemical shift change produced by each "benzene" ring of the DAN and NDI units was approximated by eq 2.[24a] The chemical shift change induced by each carbonyl of the NDI unit was approximated by eq 3.[24b] The total $\Delta\delta$ for each NDI proton under consideration (aromatic, ***c***, and ***d***) was calculated as the sum of the shifts induced by each of the two DAN "benzene" rings (eq 4). The total $\Delta\delta$ for each DAN proton under consideration (aromatic, ***j***, ***k***,and ***l***) was calculated as the sum of the shifts induced by each of the two NDI "benzene" rings and each of the four NDI carbonyls (eq 5). For methylenes, the averaged position of the two protons was used for all equations.

$$\Delta\delta_{\text{Ar ring}} = 27.6(1-3\cos^2\theta^*)/r^3 \quad (2)$$

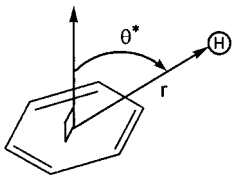

$$\Delta\delta_{\text{carbonyl}} = 9.13(G_a) - 3.08(G_b) \quad (3)$$

$$G_a = (1-3\cos^2\theta)/R_a^3$$

$$G_b = (1-3\cos^2\omega)/R_b^3$$

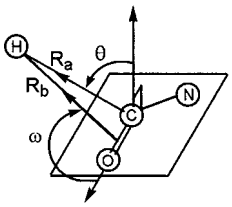

$$\Delta\delta_{\text{NDI}} = \Delta_{\text{DAN Ar ring1}} + \Delta_{\text{DAN Ar ring2}} \quad (4)$$

$$\Delta\delta_{\text{DAN}} = \Delta_{\text{NDI Ar ring1}} + \Delta_{\text{NDI Ar ring2}} + \Delta_{\text{NDI CO1}} + \Delta_{\text{NDI CO2}} + \Delta_{\text{NDI CO3}} + \Delta_{\text{NDI CO4}} \quad (5)$$

Acknowledgment. We thank the Robert A. Welch Foundation (F-1188), the National Institutes of Health (R01 GM55646), and the Alfred P. Sloan Foundation (BR-3583) for financial support of this work. We would also like to thank Mark S. Cubberley for his review of the manuscript, Steve Sorey for 2-D NMR experiments, Don O'Connor for time-resolved fluorescence measurements, and Vladimir Guelev for many lively discussions.

Supporting Information Available: Synthetic schemes and full experimental for **1**−**15**, tables of NOE data, and additional molecular modeling data. This material is available free of charge via the Internet at http://pubs.acs.org.

JA0019225

(37) HyperCube Inc., 1115 NW 4th Street, Gainesville, FL 32601.
(38) Microsoft Inc., Redmond, WA 98052.